J. Fluid Mech. (1972), *vol.* 51, *part* 4, *pp.* 687–704
Printed in Great Britain

Hydrodynamic stability in plane Poiseuille flow with finite amplitude disturbances

By W. D. GEORGE† AND J. D. HELLUMS
Rice University, Houston, Texas

(Received 23 February 1971 and in revised form 6 July 1971)

A general method for studying two-dimensional problems in hydrodynamic stability is presented and applied to the classical problem of predicting instability in plane Poiseuille flow. The disturbance stream function is expanded in a Fourier series in the axial space dimension which, on substitution into the Navier–Stokes equation, leads to a system of parabolic partial differential equations in the coefficient functions. An efficient, stable and accurate numerical method is presented for solving these equations. It is demonstrated that the numerical process is capable of accurate reproduction of known results from the linear theory of hydrodynamic stability.

Disturbances that are stable according to linear theory are shown to become unstable with the addition of finite amplitude effects. This seems to be the first work of quantitative value for disturbances of moderate and larger amplitudes. A relationship between critical amplitude and Reynolds number is reported, the form of which indicates the existence of an absolute critical Reynolds number below which an arbitrary disturbance cannot be made unstable, no matter how large its initial amplitude. The critical curve shows significantly less effect of amplitude than do those obtained by earlier workers.

1. Introduction

The prediction of instability in parallel flows is one of the most interesting problems in fluid mechanics. The very extensive literature has been reviewed elsewhere (George 1970) and several monographs are available on the subject (Lin 1955; Eckhaus 1965; Betchov & Criminale 1967). Most of the earlier work has, of course, employed the classical two-dimensional linear theory. The linear theory yields a critical Reynolds number for plane Poiseuille flow which differs significantly from the experimentally observed values although it is of the right order of magnitude.

It is generally acknowledged that the earliest stages of transition are closely related to the growth of laminar instabilities. If a disturbance in a fluid motion is initially small its growth or decay is determined by linear theory. However, if the disturbance grows, at some stage of development of the process the nonlinear terms become important and may subsequently dominate the entire process. On the other hand, if the initial disturbance is large enough, the process may be

† Present address: Getty Oil Company, Houston, Texas.

nonlinear from the beginning. Thus the question of infinitesimal versus finite disturbances is a significant one. The ability to study the development of laminar instabilities far into the nonlinear phases of the motion would be a valuable tool, which could be directed toward the goal of achieving understanding of incipient turbulent phenomena. It was our objective to develop such a tool and apply it to the classical problems of predicting instability in plane Poiseuille flow and in Poiseuille flow. The method in a general form applicable both to plane Poiseuille flow and to Poiseuille flow will be presented and discussed in §§ 3–6 below and results for plane Poiseuille flow will be presented in §§ 7 and 8. The results for Poiseuille flow will be presented in a subsequent publication.

There are several earlier papers on nonlinear effects in plane Poiseuille flow and these will be discussed below. For Poiseuille flow there has been no nonlinear prior work other than that of Dixon & Hellums (1967), which may be regarded as a qualitative study preliminary to the present work, and a recent paper by Davey & Nguyen (1971).

2. Preliminary considerations

The major obstacle in attacking the general problem by means of direct numerical integration of the equations of motion is that of dimensionality. Consider some of the problems associated with numerical integration of timewise periodic disturbances propagating downstream in an infinite channel. The flow field must in general be lengthy because instabilities of interest are typically associated with large Reynolds numbers. There is also the question of what boundary conditions to use at the downstream end of the flow field. Ideally, a disturbance should always propagate into a region of undisturbed flow but boundary conditions corresponding to this situation are difficult to impose. A further difficulty arises from the fact that any numerical process from which a quantitatively acceptable solution is to be achieved must be capable of accurate approximation of the eigenfunctions of the linear problem and their derivatives up to fourth order. These eigenfunctions vary rapidly in magnitude over certain portions of the channel, necessitating fine resolution of any computing grid in the direction perpendicular to the basic flow. Such considerations led us to restrict this work to the investigation of disturbances that are periodic in space. Virtually all earlier work in hydrodynamic stability has employed solutions constrained to be periodic in either the axial space variable or in time.

The stream function is expanded in a Fourier series containing unknown coefficients that depend upon position in the lateral channel direction and upon time. This series is inserted into the Navier–Stokes equations expressed in terms of a disturbance stream function, whereupon the collected coefficients of sine and cosine terms of the respective frequencies are separately set to zero. A system of coupled nonlinear partial differential equations for the unknown harmonic components is obtained. Integration of these equations using finite-difference techniques yields the desired solutions, whose growth or decay in time provides evidence of stability of the basic flow.

3. Mathematical formulation

In the case of plane Poiseuille flow we consider flow of a homogeneous incompressible viscous fluid in the region between two infinite stationary parallel plates. The two-dimensional fluid motion can be specified by a stream function $\psi(x, y, t)$ defined such that

$$u = \partial\psi/\partial y, \quad v = -\partial\psi/\partial x. \tag{1}$$

In dimensionless form, the function satisfies the vorticity transport equation

$$\xi_t + u\xi_x + v\xi_y = R^{-1}(\xi_{xx} + \xi_{yy}), \tag{2}$$

where

$$\xi = \psi_{xx} + \psi_{yy}. \tag{3}$$

Non-dimensionalization is based on l, the channel half-width, and on U_0, velocity of the undisturbed laminar flow at the channel centre-line. The Reynolds number is $R = (U_0 l)/\nu$.

To study the behaviour of a disturbance superimposed on the steady flow $\overline{\psi}(y)$ we substitute

$$\psi(x, y, t) = \overline{\psi}(y) + \hat{\psi}(x, y, t) \tag{4}$$

into (2) to obtain an equation for $\hat{\psi}$:

$$R^{-1}(\hat{\xi}_{xx} + \hat{\xi}_{yy}) - \hat{\xi}_t - \overline{u}\hat{\xi}_x + \overline{u}_{yy}\hat{\psi}_x = \hat{\psi}_y\hat{\xi}_x - \hat{\psi}_x\hat{\xi}_y, \tag{5}$$

in which $\hat{\xi} = \hat{\psi}_{xx} + \hat{\psi}_{yy}$ and $\overline{u} = 1 - y^2$. All terms resulting from the substitution are retained. The equations are not linearized or otherwise simplified. Substitution of the finite Fourier expansion

$$\hat{\psi}(x, y, t) = \sum_{m=0}^{M} A_m(y, t)\cos m\alpha x + B_m(y, t)\sin m\alpha x \tag{6}$$

into the stream function disturbance equation (5) leads to a system of coupled partial differential equations for the unknown coefficients $A_m(y, t)$ and $B_m(y, t)$, $m = 0, 1, \ldots, M$.

Equations that apply to flow in a cylindrical tube can readily be derived by performing manipulations analogous to those given above. The harmonic component disturbance equations for the two basic geometries can be combined conveniently into a single generalized formulation. Expressed in differential operator notation this generalization can be written as

$$\frac{\partial}{\partial t}\mathscr{L}_m[A_m] = R^{-1}\mathscr{L}_m^2[A_m] - \overline{u}m\alpha\mathscr{L}_m[B_m] + (1-\eta)\,m\alpha\overline{u}_{yy}B_m + F_m^A$$
$$\text{for} \quad m = 0, 1, 2, \ldots, M, \tag{7}$$

$$\frac{\partial}{\partial t}\mathscr{L}_m[B_m] = R^{-1}\mathscr{L}_m^2[B_m] + \overline{u}m\alpha\mathscr{L}_m[A_m] - (1-\eta)\,m\alpha\overline{u}_{yy}A_m + F_m^B$$
$$\text{for} \quad m = 1, 2, \ldots, M, \tag{8}$$

$$F_m^A = -\tfrac{1}{2}\alpha\theta\hat{F}_m^A, \quad F_m^B = -\tfrac{1}{2}\alpha\theta\hat{F}_m^B, \tag{9}$$

$$\theta = 1 + \eta(1/y - 1), \tag{10}$$

$$F_0^A = \sum_{p=1}^{M} Q_{pp}, \tag{11}$$

$$\hat{F}_m^A = 2m\left\{A_0'\mathscr{L}_m[B_m] - B_m\frac{\partial}{\partial y}\mathscr{L}_0[A_0]\right\} + \sum_{p=1}^{M-m}\{Q_{(m+p)p} + Q_{p(m+p)}\} + \sum_{p=1}^{m-1}R_{(m-p)p}, \quad (12)$$

$$F_m^B = 2m\left\{A_m\frac{\partial}{\partial y}\mathscr{L}_0[A_0] - A_0'\mathscr{L}_m[A_m]\right\} + \sum_{p=1}^{M-m}\{S_{(m+p)p} - S_{p(m+p)}\} + \sum_{p=1}^{m-1}T_{(m-p)p}, \quad (13)$$

where

$$\left.\begin{aligned} Q_{qp} &= E_{qp} + H_{qp}, \quad R_{qp} = E_{qp} - H_{qp}, \\ S_{qp} &= G_{qp} - F_{qp}, \quad T_{qp} = G_{qp} + F_{qp}; \end{aligned}\right\} \quad (14)$$

$$\left.\begin{aligned} E_{qp} &= pA_q'\mathscr{L}_q[B_q] - q\mathscr{S}_p[A_p]\,B_q, \\ F_{qp} &= -pA_q'\mathscr{L}_q[A_q] - q\mathscr{S}_p[B_p]\,B_q, \\ G_{qp} &= pB_q'\mathscr{L}_q[B_q] + q\mathscr{S}_p[A_p]\,A_q, \\ H_{qp} &= -pB_q'\mathscr{L}_q[A_q] + q\mathscr{S}_p[B_p]\,A_q; \end{aligned}\right\} \quad (15)$$

$$\mathscr{L}_m = \frac{\partial^2}{\partial y^2} - \frac{\eta}{y}\frac{\partial}{\partial y} - (m\alpha)^2; \quad (16)$$

$$\mathscr{S}_m = \frac{\partial}{\partial y}\mathscr{L}_m - \frac{2\eta}{y}\mathscr{L}_m; \quad (17)$$

$$\bar{u} = 1 - y^2; \quad (18)$$

$$\eta = \begin{cases} 0 \text{ for plane Poiseuille flow,} \\ 1 \text{ for Poiseuille flow.} \end{cases} \quad (19)$$

In plane Poiseuille flow the conditions that the velocities vanish on the boundaries may be expressed in terms of the harmonic components as indicated below:

$$\left.\begin{aligned} A_m(\pm 1) &= \partial A_m(\pm 1)/\partial y = 0, \\ B_m(\pm 1) &= \partial B_m(\pm 1)/\partial y = 0. \end{aligned}\right\} \quad (20)$$

Note that the only unstable eigenfunctions that exist according to linear theory are those that are even functions of y with respect to stream function. For this reason we will concentrate on nonlinear problems in which the fundamental fluctuation is an even function. Of course the solutions are not constrained to be even. It can be shown that an initially even function for A_1 will remain even for all time, the nonlinear interactions being completely consistent with this assertion. The equations also dictate that alternate harmonics are of opposite parity. Thus we can reduce the required computer time by a factor of two by solving the problem over only half the channel using the following centre-line boundary condition:

$$\left.\begin{aligned} A_m(0) &= A_m''(0) = 0 \quad \text{for } m \text{ even}, \\ A_m'(0) &= A_m'''(0) = 0 \quad \text{for } m \text{ odd}. \end{aligned}\right\} \quad (21)$$

Since the initial condition on A_1 is even, all the odd harmonics, $A_1, A_3, \ldots$, will be even functions; the even harmonics, $A_0, A_2, \ldots$, will be odd functions.

For Poiseuille flow it is not possible to argue that the various harmonics are odd or even. The conditions are that the velocity vanish at the boundary and that we have symmetry and a bounded solution at the centre-line. The boundary conditions imply constant mass flow.

4. Numerical approximation and solution

For computational purposes it is convenient to express (7) and (8) directly in terms of the derivatives of A_m and B_m. This is accomplished by substitution of the differential operator (16) into (7) and (8). Upon simplification this yields

$$\gamma_4 A_m^{\text{iv}} + \gamma_3 A_m''' + \gamma_2 A_m'' + \gamma_1 A_m' + \gamma_0 A_m + \lambda_0 \partial A_m/\partial t + \lambda_1 \partial A_m'/\partial t + \lambda_2 \partial A_m''/\partial t + \sigma D_m + \tau B_m = F_m^A, \quad (22)$$

$$\gamma_4 B_m^{\text{iv}} + \gamma_3 B_m''' + \gamma_2 B_m'' + \gamma_1 B_m' + \gamma_0 B_m + \lambda_0 \partial B_m/\partial t + \lambda_1 \partial B_m'/\partial t + \lambda_2 \partial B_m''/\partial t - \sigma C_m - \tau A_m = F_m^B, \quad (23)$$

where

$$\left.\begin{aligned} C_m &= A_m'' - \lambda_1 A_m' - (m\alpha)^2 A_m, \\ D_m &= B_m'' - \lambda_1 B_m'' - (m\alpha)^2 B_m. \end{aligned}\right\} \quad (24)$$

The primes denote differentiation with respect to y (r for Poiseuille flow).

Define

$$\gamma_i = R^{-1}\hat{\gamma}_i, \quad (25)$$

then

$$\left.\begin{aligned} &\hat{\gamma}_4 = 1, \quad \hat{\gamma}_3 = -\eta(2/y), \quad \hat{\gamma}_2 = -2(m\alpha)^2 + \eta(3/y^2), \\ &\hat{\gamma}_1 = -\eta\hat{\gamma}_2/y, \quad \hat{\gamma}_0 = (m\alpha)^4, \\ &\lambda_0 = (m\alpha)^2, \quad \lambda_1 = \eta/y, \quad \lambda_2 = -1, \\ &\sigma = -\bar{u}m\alpha, \quad \tau = (1-\eta)\bar{u}_{yy}m\alpha, \quad \bar{u} = 1 - y^2, \\ &\eta = \begin{cases} 0 \text{ for plane Poiseuille flow,} \\ 1 \text{ for Poiseuille flow.} \end{cases} \end{aligned}\right\} \quad (26)$$

Equations (22) and (23) were discretized using Crank–Nicolson differencing in time. That is, knowing A_m and B_m at the nth time step, to advance to the $(n+1)$th step we take all terms other than the time derivatives to be the average of the values at the two time levels. The Crank–Nicolson approach is characterized by a small time truncation error and is known to be numerically stable in simpler problems for which the theory of numerical stability is well developed. Fourth-order space differencing was employed, so we expect an overall truncation error of order $\{(\Delta y)^4 + (\Delta t)^2\}$.

We define the difference operators

$$\left.\begin{aligned} \delta_t Q_j &= [Q_j^{(n+1)} - Q_j^{(n)}]/\Delta t, \\ \delta_y Q_j &= [Q_{j-2} - 8Q_{j-1} + 8Q_{j+1} - Q_{j+2}]/12/h, \\ \delta_y^2 Q_j &= [-Q_{j-2} + 16Q_{j-1} - 30Q_j + 16Q_{j+1} - Q_{j+2}]/12h^2, \\ \delta_y^3 Q_j &= [-Q_{j-2} + 2Q_{j-1} - 2Q_{j+1} + Q_{j+2}]/2h^3, \\ \delta_y^4 Q_j &= [Q_{j-2} - 4Q_{j-1} + 6Q_j - 4Q_{j+1} + Q_{j+2}]/h^4, \end{aligned}\right\} \quad (27)$$

where $h \equiv \Delta y$. The difference operators δ_y and δ_y^2 have error terms of order h^4, whereas the error terms for δ_y^3 and δ_y^4 are of order h^2. Since fourth-order difference expressions for third and fourth derivatives involve seven grid points it would be necessary to solve a set of linear algebraic equations having hepta-diagonal matrix forms. Hepta-diagonal systems require 50 % more computing time to solve than penta-diagonal systems. For this reason we decided to use lower order implicit approximations for high derivatives. However, we were able to raise the overall accuracy to h^4 by including error terms for the high derivatives. The error terms are evaluated explicitly and included in the right-hand side of the resulting linear algebraic equations. In other words the error terms are evaluated at the 'nth' or known time level and hence cause no complication in the algebraic procedure. These error terms are actually the first neglected non-vanishing terms from the Taylor expansions. They involve the difference approximations to the fifth and sixth derivatives of the dependent variables. The error terms remain small throughout the solution and do not vary greatly with time. Hence, little or no accuracy is lost in treating them explicitly rather than implicitly. This method of improving accuracy with no additional computation seems to be novel and it is a very important feature of the method. With this correction it will be shown below that far fewer subdivisions are required to achieve any specified level of accuracy. Complete details of the procedure and results are available (George 1970).

We are now in a position to write down the Crank–Nicolson difference equation corresponding to equation (22) for $A_{m(j)}$. The notation $A_{m(j)}^{(m+1,k)}$ refers to the kth iterate of the mth harmonic A_m evaluated at the jth grid point (or spatial position $y = jh$) at the time level $t = (n+1)\,\Delta t$. Define the averaging operator

$$\mathscr{A}[Q^{(n)}] = \tfrac{1}{2}[Q^{(n+1)} + Q^{(n)}]. \tag{28}$$

The difference equations for the $A_{m(j)}$ are then

$$\sum_{i=0}^{4} \gamma_{i(j)}\,\mathscr{A}[\delta_y^i A_{m(j)}^{(n,k+1)}] + \sum_{i=0}^{2} \lambda_{i(j)}\,\delta_t\,\delta_y^i A_{m(j)}^{(n,k+1)}$$
$$= -\sigma_{(j)}\,\mathscr{A}[D_{m(j)}^{(n,k)}] - \tau_{(j)}\,\mathscr{A}[B_{m(j)}^{(n,k)}] + \mathscr{A}[F_{m(j)}^{A(n,k)}] - \gamma_{4(j)}\,E_m^{\mathrm{iv}(n)} - \gamma_{3(j)}\,E_m^{'''(n)}, \tag{29}$$

where
$$E_m^{\mathrm{iv}} = -\tfrac{1}{6}h^2 A_m^{\mathrm{vi}}, \quad E_m^{'''} = -\tfrac{1}{4}h^2 A_m^{\mathrm{v}}. \tag{30}$$

Direct substitution and subsequent algebraic manipulations lead to a set of nonlinear algebraic equations. These equations and an analogous set for the $B_{m(j)}$ are solved by iteration with respect to the nonlinear coupling terms. This task is accomplished by considering the set of finite-difference equations in cyclic order. For each individual equation the nonlinear terms are explicitly evaluated using the latest available updated values of the dependent variables. These terms are then added to the already known iteration invariant parts of the right-hand side. Finally, the resultant set of linear algebraic equations are solved for new values of either $A_{m(j)}$ or $B_{m(j)}$. The process is repeated until certain convergence criteria, defined later, are satisfied. The iteration process is feasible because changes in the nonlinear terms corresponding to fairly large values of time increment are small to moderate in magnitude, so that the computation can proceed at a reasonably rapid pace with little penalty regarding the number of iterations required for convergence.

Numerical experimentation was carried out to explore the possibility of letting the nonlinear terms lag one time step or even updating them only on the first few iterations, but we experienced inferior performance with respect to stability and accuracy. The motivation was, of course, to reduce the computational requirements since a large portion of time is spent evaluating the nonlinear terms, particularly when a large number of harmonics were retained.

The algebraic equations are

$$[N^-_{m(j)}]\,A^{(n+1\,k+1)}_{m(j-2)} + [P^-_{m(j)}]\,A^{(n+1,k+1)}_{m(j-1)} + [Q_{m(j)}]\,A^{(n+1,k+1)}_{m(j)} + [P^+_{m(j)}]A^{(n+1,k+1)}_{m(j+1)} + [N^+_{m(j)}]\,A^{(n+1,k+1)}_{m(j+2)} = H^{(n)}_{m(j)} + Y^{(n+1,k)}_{m(j)} \tag{31}$$

and

$$[N^-_{m(j)}]\,B^{(n+1,k+1)}_{m(j-2)} + [P^-_{m(j)}]\,B^{(n+1,k+1)}_{m(j-1)} + [Q_{m(j)}]\,B^{(n+1k+1)}_{(mj)} + [P^+_{m(j)}]\,B^{m(j+1)}_{(n+1,k+1)} + [N^+_{m(j)}]\,B^{(n+1,k+1)}_{m(j+2)} = G^{(n)}_{m(j)} + Z^{(n+1,k)}_{m(j)}, \tag{32}$$

where

$$\left.\begin{aligned}
N^-_{m(j)} &= 1-\tfrac{1}{2}\hat\gamma_3 h+\tfrac{1}{12}h^2[\hat\gamma_1 h-\hat\gamma_2]+\tfrac{1}{6}\theta[\lambda_1 h-\lambda_2],\\
P^-_{m(j)} &= -4+\hat\gamma_3 h+\tfrac{2}{3}h^2[2\hat\gamma_2-\hat\gamma_1 h]+\tfrac{4}{3}\theta[2\lambda_2-\lambda_1 h],\\
Q_{m(j)} &= 6-\tfrac{5}{2}\hat\gamma_2 h^2+\hat\gamma_0 h^4+\theta[2\hat\lambda_0 h^2-5\lambda_2],\\
P^+_{m(j)} &= -4-\hat\gamma_3 h+\tfrac{2}{3}h^2[2\hat\gamma_2+\hat\gamma_1 h]+\tfrac{4}{3}\theta[2\lambda_2+\lambda_1 h],\\
N^+_{m(j)} &= 1+\tfrac{1}{2}\hat\lambda_3-\tfrac{1}{12}h^2[\hat\gamma_1 h+\hat\gamma_2]-\tfrac{1}{6}\theta[\lambda_1 h+\lambda_2],\\
H^{(n)}_{m(j)} &= -\hat N^-_{m(j)}A^-_{m(j-2)}-\hat N^+_{m(j)}A^n_{m(j+2)}-\hat P^-_{m(j)}A^{(n)}_{m(j-1)}-\hat P^+_{m(j)}A^{(n)}_{m(j+1)}-\hat Q_{m(j)}A^{(n)}_{m(j)}\\
&\quad +\hat R^-_{m(j)}A^{(n)}_{m(j-3)}+\hat R^+_{m(j)}A_{m(j+3)},\\
\text{and}\quad \theta &= (Rh^2)/(\Delta t),\\
Y_{m(j)} &= Rh^4[F^A_{m(j)}-\sigma D_{m(j)}-\tau B_{m(j)}],\\
\hat N^-_{m(j)} &= 1-\tfrac{1}{2}\hat\gamma_3 h+\tfrac{1}{12}h^2[\hat\gamma_1 h-\hat\gamma_2]-\tfrac{1}{6}\theta[\lambda_1 h-\lambda_2]+[\hat\gamma_3 h-2],\\
\hat P^-_{m(j)} &= -4+\hat\gamma_3 h+\tfrac{2}{3}h^2[2\hat\gamma_2-\hat\gamma_1 h]-\tfrac{4}{3}\theta[2\lambda_2-\lambda_1 h]+[5-\tfrac{5}{4}\hat\gamma_3 h],\\
\hat Q_{m(j)} &= 6-\tfrac{5}{2}\hat\gamma_2 h^2+\hat\gamma_0 h^4-\theta[2\lambda_0 h^2-5\lambda_2]-\tfrac{20}{3},\\
\hat P^+_{m(j)} &= -4-\hat\gamma_3 h+\tfrac{2}{3}h^2[2\hat\gamma_2+\hat\gamma_1 h]-\tfrac{4}{3}\theta[2\lambda_2+\lambda_1 h]+[5+\tfrac{5}{4}\hat\gamma_3 h],\\
\hat N^+_{m(j)} &= 1+\tfrac{1}{2}\hat\gamma_3 h-\tfrac{1}{12}h^2[\hat\gamma_1 h+\hat\gamma_2]+\tfrac{1}{6}\theta[\lambda_1 h+\lambda_2]-[2+\hat\gamma_3 h],\\
\hat R^-_{m(j)} &= \tfrac{1}{3}-\tfrac{1}{4}\hat\gamma_3 h,\quad \hat R^+_{m(j)} = \tfrac{1}{3}+\tfrac{1}{4}\hat\gamma_3 h,\\
G^{(n)}_{m(j)} &= -\hat N^-_{m(j)}B^{(n)}_{m(j-2)}-\hat N^+_{m(j)}B^{(n)}_{m(j+2)}-\hat P^-_{m(j)}B^{(n)}_{m(j-1)}-\hat P^+_{m(j)}B^{(n)}_{m(j+1)}-\hat Q_{m(j)}B^{(n)}_{m(j)}\\
&\quad +\hat R^-_{m(j)}B^{(n)}_{m(j-3)}+\hat R^+_{m(j)}A_{m(j+3)},\\
Z_{m(j)} &= Rh^4[F^B_{m(j)}+\sigma C_{m(j)}+\tau A_{m(j)}].
\end{aligned}\right\} \tag{33}$$

The **N**, **P** and **Q** coefficients are time invariant and depend only on Reynolds number, wavenumber, y, Δy and Δt; accordingly, they need only be evaluated once, during the initial phase. For plane Poiseuille flow **N**, **P** and **Q** do not depend on y and thus reduce to constants. The **G** and **H** coefficients must be evaluated once each time step, while the coefficients containing the updated nonlinear terms at the advanced time level must be re-evaluated at each iteration.

Finally, the algorithm for solving penta-diagonal systems of linear algebraic equations $\mathbf{AX} = \mathbf{F}$ is accomplished by factorizing $\mathbf{A}$ into a lower-triangular band matrix $\mathbf{L}$ and an upper-triangular band matrix $\mathbf{U}$,

$$\mathbf{A} = \mathbf{LU}, \tag{34}$$

and solving, in order, the equations

$$\mathbf{L\lambda} = \mathbf{F}, \tag{35}$$

$$\mathbf{UX} = \mathbf{\lambda}. \tag{36}$$

Because of their triangular nature, the solution of (35) and (36) is easy; solution of (35) takes place in the order of increasing j, while solution of (36) is performed in order of decreasing j. The factorization phase requires $8N$ arithmetic operations and need only be done once since matrix **A** is independent of time. The forward and back substitution phases each require $4N$ operations and must be accomplished for each iteration for each harmonic in ascending sequence.

The iteration criterion used was

$$\max_{m} \left\{ \frac{\max_{j} |A_{m(j)}^{(n+1,k+1)} - A_{m(j)}^{(n+1,k)}|}{\max_{j} |A_{m(j)}^{(n+1,k+1)}|} \right\} < 10^{-6}. \tag{37}$$

A similar condition on $B_{m(j)}^{(n+1)}$ was required simultaneously. The condition corresponds roughly to a requirement that all of the quantities $A_{m(j)}^{(n+1)}$ and $B_{m(j)}^{(n+1)}$ have changed by no more than one digit in the sixth significant figure during the preceding iteration.

5. Comparison of computational methods

Recently, two other expansion methods for solving spatially periodic hydrodynamic stability problems have been reported in the literature. We thought it worthwhile to compare the computational effort required of these methods with that of the method used in this investigation.

Dowell (1969) proposed to discretize only the lateral space variable by means of a Galerkin procedure, leaving the time variable continuous. The solution was expanded into a subset of a larger class of functions which satisfied the boundary conditions and which constituted a complete but non-orthogonal set. The unknown expansion coefficients were determined so that the linear combination minimized a measure of error with respect to satisfaction of the equations, which led to a complicated system of ordinary differential equations. The work required to solve these equations was large since the nonlinear terms were represented by four-fold summation terms which had to be evaluated at least twice per time step. For comparative purposes we took as a convenient and most reasonable basis the case involving a mean flow and three fluctuating harmonics with forty expansion modes. Dowell reported that, typically, forty modes were required for convergence of the series for solution of the linear problem.

Pekeris & Shkoller (1969*a*) studied periodic disturbances of finite amplitude by expanding the stream function into a series of eigenfunctions and adjoint eigenfunctions of the associated linear problem. Again a system of ordinary differential equations is obtained and once more a large amount of work is involved. First, one must compute the first twenty-one eigenfunctions and adjoint eigenfunctions for each of three harmonics. This is in itself a task of major proportions which must be repeated for each wavenumber, Reynolds number combination, and for each geometrical situation. Next, all of the interaction coefficients, complex integral functions of the eigenfunctions and adjoint eigenfunctions must be obtained. This constitutes a second major computational task since over 200000 complex coefficients are involved. Finally, 123 simultaneous ordinary differential equations must be integrated forward in time.

The finite-difference method of solution proposed in this paper requires far less computational effort and far less storage than the two methods just described.

The main reason is that no expansions are made in the lateral spatial dimension. These lateral expansions yield very large numbers of nonlinear interaction terms. The comparison shown below (table 1) does not include computation of indices, fetch and storage of elements of arrays, or various other book-keeping functions. However, the estimates for all three methods are made on the same basis using the number of terms in each series recommended by the authors.

	Operations/step $\times 10^{-6}$	Memory requirement in words $\times 10^{-6}$
Dowell	100·0	16·4
Pekeris & Shkoller	6·23	0·4
This work	0·164	0·005

TABLE 1

The results presented here do not imply that the Galerkin approach to problems of this type is without promise. In fact, we believe the Galerkin approach is highly promising if basis functions with less total support are selected.

6. Computational aspects

All calculations were carried out on the Burroughs B-5500 computer which is characterized by a 48 bit word, 4 μs memory access time and 2 μs fixed-point add time. Solutions to linear problems were obtained at a rate of 0·7 s per time step or, equivalently, 86 steps per minute.

Nonlinear problems for which two fluctuating harmonics were retained required about 4–4·5 s per time step depending on the number of iterations needed for convergence. Usually four or five iterations were sufficient but more were taken in a few situations in which the solution was rapidly changing relative to the size of the time increment. A dimensionless time increment of 0·3 was used for all problems except for very high amplitude cases in which the larger size of the second harmonic made it necessary to reduce the time increment. Computational runs were usually made to a time of 100 although in several cases times of 200 to 230 were used. Most nonlinear runs required from 45 min to 1 h to complete. The use of more harmonics increased the computer time since each additional harmonic involves two additional partial differential equations and additional nonlinear terms in all equations. Also, the higher harmonics possess shorter periods necessitating use of smaller time increments. Use of four harmonics, for example, required about five times as much computer time as a two-harmonic problem. Here nine equations were involved as opposed to five. Also, the time step must be halved since the period of the fourth harmonic is half that of the second harmonic. Studies indicated that at least twenty steps per cycle are needed to maintain numerical stability.

To put the computer time requirement into proper perspective it must be pointed out that the computer used in this work is relatively slow. Large computers of recent design operate about two orders of magnitude faster than the B-5500.

7. Linear studies

We have demonstrated the validity of the method by solving a large number of problems involving small disturbances, using a wide variety of combinations of wavenumber and Reynolds number. The results have been compared with analogous results obtained by previous workers. In the process, we also have studied the effect of space and time increment sizes on accuracy and stability of the numerical solutions.

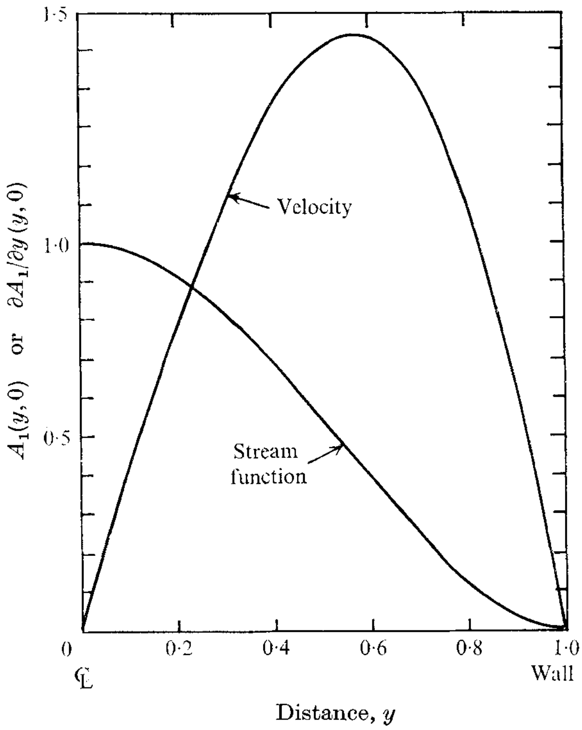

FIGURE 1. Initial stream function and velocity fluctuations for $K_A = 1$.

Initial conditions consisted of a fundamental disturbance having the shape of the first symmetric eigenfunction of a closely related problem, Chandrasekhar (1961). This function, $f(y)$, has a shape somewhat similar to the real part of the least stable eigenfunction arising from linear theory. The stream function and velocity fluctuations corresponding to $f(y)$ are shown in figure 1. The initial conditions used were

$$A_1(y,0) = K_A\, f(y),$$
$$A_m(y,0) = 0 \quad \text{for} \quad m \neq 1,$$
$$B_m(y,0) = 0 \quad \text{for all } m,$$

where K_A is the specified initial amplitude.

For problems that are solely linear only $A_1(y,t)$ and $B_1(y,t)$ are involved, there being no interaction between the fundamental fluctuation and itself, the mean flow or higher harmonics. Solutions to the Orr–Sommerfeld equations are often expressed in the form

$$\psi(x,y,t) = \phi(y)\, e^{i\alpha(x+ct)}.$$

We have written our solutions in the form

$$\psi(x,y,t) = A(y,t)\cos\alpha x + B(y,t)\sin\alpha x.$$

The correspondence between the two forms is such that

$$A(y,t) = (\phi_r \cos\alpha c_r t - \phi_i \sin\alpha c_r t)\, e^{\alpha c_i t},$$
$$B(y,t) = -(\phi_i \cos\alpha c_r t + \phi_r \sin\alpha c_r t)\, e^{\alpha c_i t}.$$

The linear solutions are sinusoidal with period $2\pi/(\alpha c_r)$ and growth or decay rate $e^{\alpha c_i t}$. The complex eigenvalue c has been obtained by various workers as a function of α and R. Therefore we have a means of comparing computed solutions with earlier work. As an example, in figure 2 we show the oscillation computed

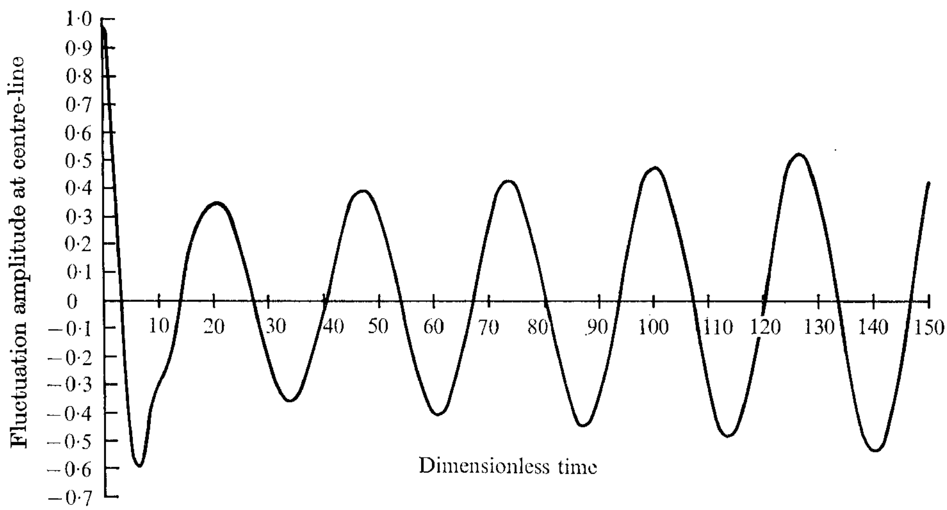

FIGURE 2. Computed linear oscillation ($\alpha = 1$, $R = 10\,000$). $A(0,t) = \exp(c_i t)\cos(c_r t)$ with $c_i = 0{\cdot}003758$, $c_r = 0{\cdot}2374$.

for $\alpha = 1$, $R = 10\,000$. Following the initial transient, a pure sine wave is obtained which is characterized by period and growth rate parameters that are in exact agreement with previous work. We found also that the corresponding eigenfunction extracted from our results agrees well with the results of Thomas (1953). The maximum deviation is about 2 % and this occurs very near the wall, where the eigenfunction itself is very small. At the centre-line the error is about 0·004 %.

The effect of varying the grid size is shown in figure 3. Clearly, the quality of the results deteriorates as the number of intervals decreases until the method fails completely. The enhancing of solution quality is dramatic when steps are taken to achieve fourth-order accuracy, as discussed previously. This simple device provides a very important contribution to the efficiency of the method. We note that more than 200 intervals are required to achieve the same accuracy using second-order methods as can be achieved with only 50 intervals using the fourth-order method. It is important to note that the more accurate solutions are obtained with little or no increase in computing time.

A number of linear problems were solved holding the space increment fixed at 0·02 and varying the time step. It was determined that period and growth rate were not affected to four or five significant figures by increasing the step size by a factor of two, four or eight. The number of iterations required for convergence did, however, increase significantly, doubling and even trebling until finally no solution at all could be obtained. We found that a time step corresponding to about 20 intervals for each cycle in time of the solution was optimum. For non-linear problems this criterion was applied to the highest harmonic in choosing an appropriate step size.

Orr–Sommerfeld eigenvalues were computed for a variety of problems with Reynolds numbers ranging up to 100000. We invariably obtained values that were within the accuracy to which we could determine known linear results from the literature. The complete success that we had in verifying linear theory over a wide range of α–R combinations gave us confidence in the numerical procedure which was then applied to nonlinear problems.

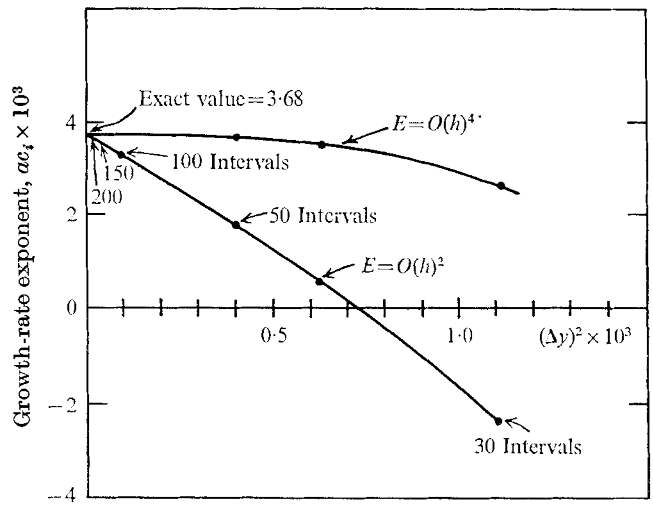

FIGURE 3. The effect of channel resolution on the accuracy of linear solutions ($\alpha = 1$, $R = 10000$).

8. Nonlinear studies

The behaviour of finite amplitude disturbances was for the most part studied using the mean flow and two harmonics. The fundamental or first harmonic (A_1) alone was initially non-zero. This harmonic interacts with itself to create an associated Reynolds stress which excites both the zeroth and second harmonics thus inducing a distortion of the mean flow. Subsequent interactions of the harmonics may cause instability to occur at Reynolds numbers lower than the critical value predicted by linear theory. The solutions shown in figure 4 illustrate such an occurrence. The oscillation, which represents the stream function disturbance as shown in figure 1 with an initial amplitude K_A of 0·10, is characterized by rapid and sustained growth after an initial transient. Also shown is the bounding envelope of maxima and minima of the oscillating disturbance for the equivalent linear problem. The parameters used correspond to a point in the α, R plane near the apex of the neutral curve but just inside the stable or subcritical region. We thus observe that finite amplitude instability does indeed exist for a situation where flow is stable according to linear theory. A similar calculation was made in which a linearly unstable flow ($\alpha = 1$, $R = 7000$) was shown to become even more unstable with the addition of nonlinearity. The growth rate exponent, $c_i = 7{\cdot}93 \times 10^{-3}$, is almost four times that of the linear problem ($2{\cdot}0 \times 10^{-3}$) and is in fact larger than the maximum possible linear value of $7{\cdot}65 \times 10^{-3}$.

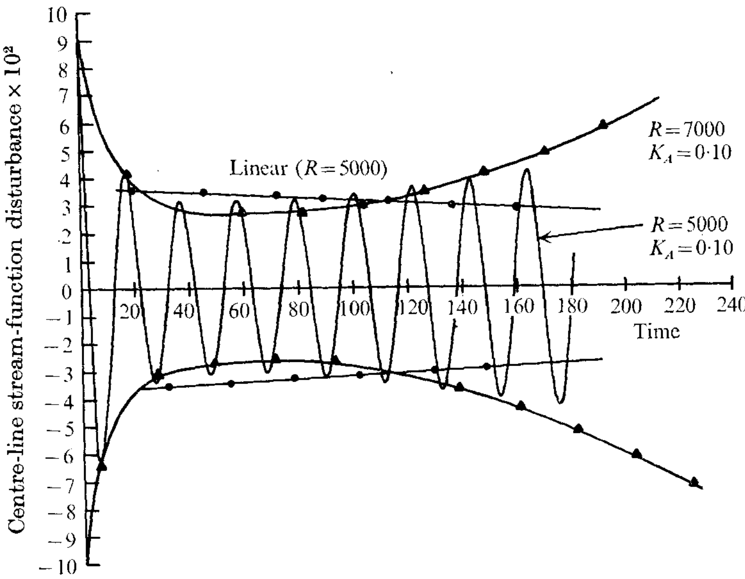

FIGURE 4. Illustration of the effect of nonlinear terms on stability ($\alpha = 1$).

We show in figure 5 curves representing solutions for a sequence of Reynolds numbers ranging through the neutral curve, all obtained using unit wavenumber and 0·10 initial amplitude. To simplify the interpretation the amplitude of the fluctuation is presented rather than the complete wave. The critical Reynolds number is reduced from 5815 to about 4125. Similar reductions will be associated with each wavenumber and amplitude. The disturbance shape also presumably has an effect. Another interpretation would be to associate a critical equilibrium amplitude with each point in the subcritical portion of the α, R plane.

Analogous sets of solution curves to those given in figure 5 were generated for a variety of initial amplitudes ranging from 0·02 to 0·30. Careful interpretation of these curves allowed construction of a curve relating Reynolds number to critical amplitude but valid only for disturbances having an imposed fundamental wavelength of 2π ($\alpha = 1$). Nonlinear neutral Reynolds numbers were found by obtaining some measure of late-time slope for each solution as a function of R and interpolating to zero growth rate. Repetition of the process for the sequence of initial amplitudes led to figure 6, which shows the effect of amplitude on neutral Reynolds numbers. The most striking characteristic of the curve is the existence of an absolute minimum Reynolds number below which the flow cannot be rendered unstable – no matter how large the initial amplitude. Also notable is the fact that nonlinear growth is limited to amplitudes slightly in excess of 0·20.

Hence, the portion of the curve to the right of the minimum represents equilibrium amplitudes. Amplitudes higher than those on this portion of the curve decay, while amplitudes lower than those on this portion of the curve grow, provided the Reynolds number is higher than the minimum.

An experimentally determined critical Reynolds number for reverse transition, that is, the smallest Reynolds number for which fully developed turbulent flow can be maintained in a two-dimensional channel, has been shown to be about 2100 by several workers. This figure is consistent with the results of our computations which yield a value of about 3500, obtained for a single disturbance.

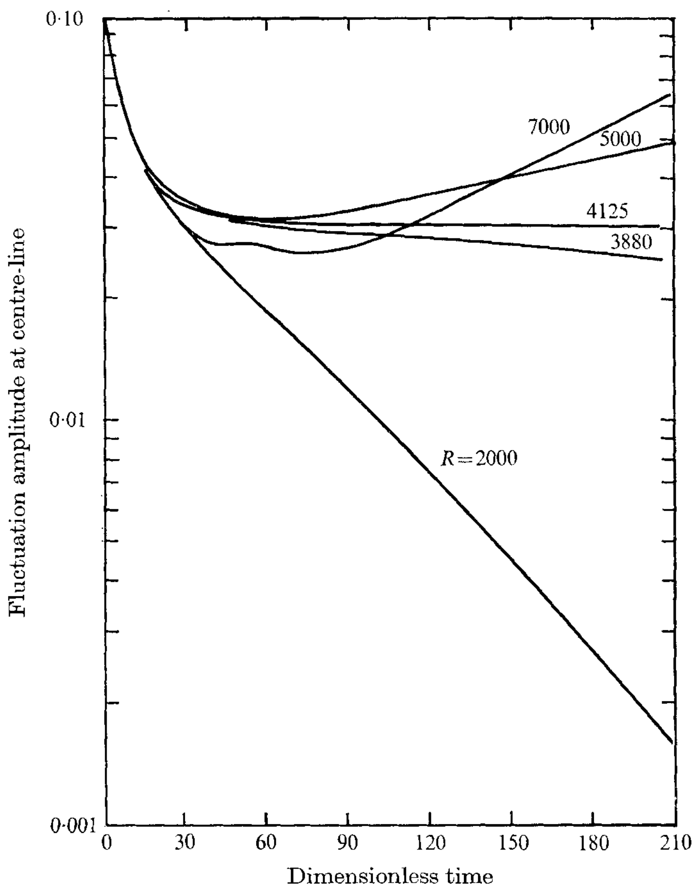

FIGURE 5. The effect of Reynolds number on nonlinear solutions ($\alpha = 1$, $K_A = 0{\cdot}10$).

It would be desirable to construct curves of critical Reynolds number versus amplitude for many values of α and various disturbance shapes. The outer locus of points on such curves would yield a critical Reynolds number–amplitude relationship closely akin to the experimental situation in which a variety of disturbances are present. The minimum of the envelope of these curves would be lower than the Reynolds number of 3500 found for $\alpha = 1$ and would presumably be close to the experimentally observed range.

A comparison of our critical curve with those obtained by earlier workers (adjusted to correspond to our basis of amplitude specification and Reynolds number) is given in figure 7. The comparison is restricted to lower amplitudes than the previous figure since previous work is not expected to be valid at higher amplitudes. A much less drastic effect of amplitude is indicated by our results than those obtained by methods valid only for small amplitude. Pekeris's two relations (Pekeris & Shkoller 1969*a*, *b*) were presented in companion papers and are inexplicably at variance with one another. The lower curve of the two seems to be less reliable. It is from the work discussed previously. In comparisons with Pekeris's work it should be noted that K_A is twice the amplitude parameter λ_c used by Pekeris. It is interesting and rather surprising to note that the first nonlinear

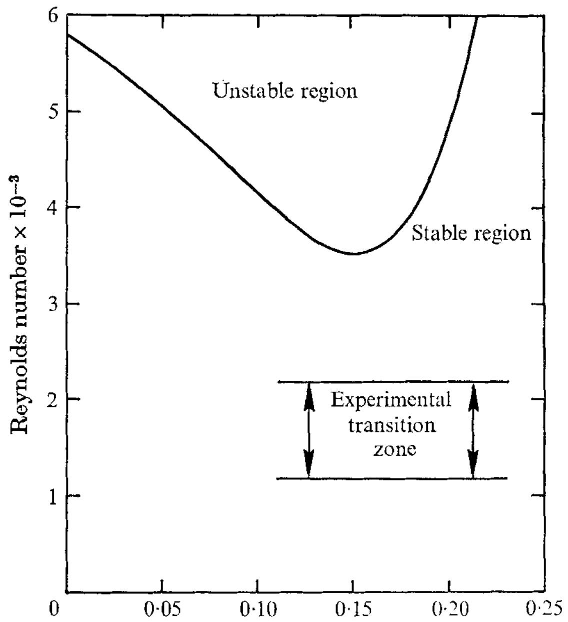

FIGURE 6. Critical behaviour for finite amplitude disturbances ($\alpha = 1$).

work (Meksyn & Stuart 1951) gave the best estimate of the effect of amplitude until the present work. However, at the time of that first work the starting point, the linear theory, was not in agreement with the currently accepted value.

Most runs were made using two harmonics but several studies were made on the effect of higher harmonics. The magnitude of the second harmonic always increases with time from zero to an early maximum and then decreases. The function may ultimately increase in the unstable cases but the decrease is continuous for stable situations. The absolute maximum is a well-defined function of amplitude and does not seem to depend significantly on Reynolds number, at least in the neighbourhood of the neutral curve. For $K_A = 0{\cdot}02$, the maximum magnitude of the second harmonic is always two orders of magnitude less than the first harmonic. The overall trend is shown in figure 8. Even for the largest amplitude, 0·3, the second harmonic is bounded by 0·029, or less than 10% of the initial amplitude. Hence, it appears that two harmonics give adequate accuracy. The runs using four harmonics seemed to be slightly more stable than the corresponding two harmonic cases. For example, with $K_A = 0{\cdot}20$ and $R = 3500$ the results were similar to the results obtained with the same K_A for $R = 3000$ and two harmonics.

It should be emphasized that the effect of adding the third and fourth harmonics was slight even for high amplitudes. For the case mentioned above, $K_A = 0{\cdot}20$, the second, third and fourth harmonic amplitudes were always less than 0·017, 0·003 and 0·0015 respectively. The fundamental harmonic amplitude

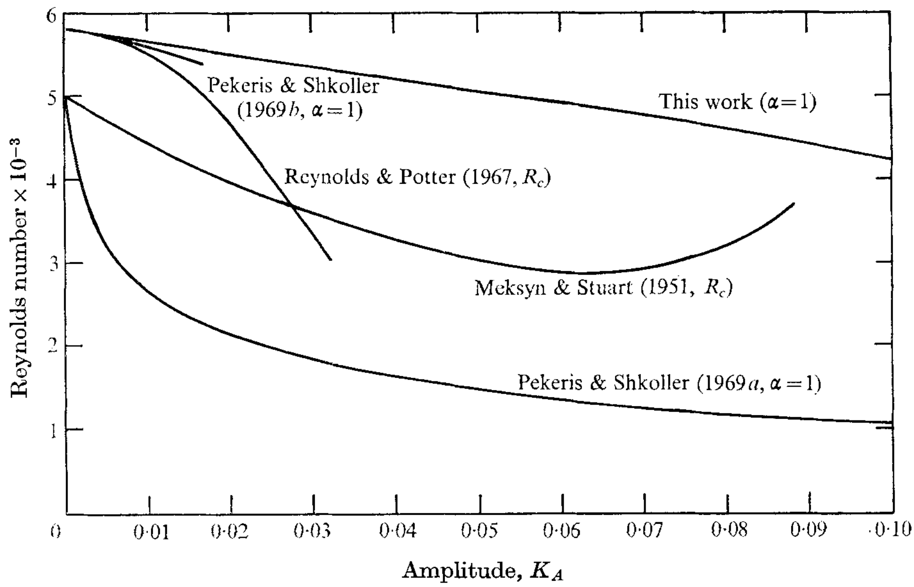

FIGURE 7. Comparison of critical curve with earlier work.

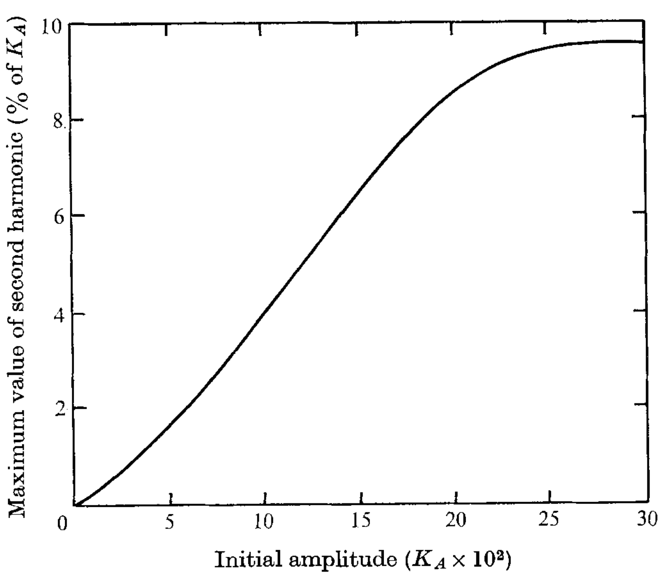

FIGURE 8. The effect of initial amplitude on the maximum magnitude of the second harmonic.

of course started at 0·20 in terms of the stream function or 0·3 in terms of velocity. That is to say, the initial velocity deviated from the parabolic initial profile by 0·3 of the maximum velocity. Therefore, even for this very large disturbance the higher harmonics seem to be negligible although, of course, this simple observation of magnitude of the harmonics is not conclusive proof. For smaller initial disturbances, the higher harmonics are a much smaller fraction of the fundamental harmonic as indicated above.

In the unstable cases the velocity profile apparently tends to develop a reversal in curvature. Consider the unstable case of $K_A = 0{\cdot}20$ and $R = 4000$ at a time of $t = 147$. At this stage of development A_0 has developed from a zero initial value to a maximum magnitude of 0·0080 and the mean velocity deviates from the undisturbed profile by a maximum of 0·033. The second derivative of the mean velocity profile ranges from $-3{\cdot}44$ at $r = 0{\cdot}68$ to $3{\cdot}88$ at $r = 0{\cdot}92$, with a change in sign at $r = 0{\cdot}86$. Initially the second derivative of the mean velocity profile is -2 at all positions.

9. Conclusion

We have developed a practical and efficient numerical method for obtaining solutions to the equations of motion pertaining to two-dimensional disturbances superimposed on laminar flow. The numerical process was shown to be stable and accurate when applied to problems of linear plane Poiseuille flow. Orr–Sommerfeld eigenvalues were computed to a high enough degree of accuracy to be considered exact, using only fifty channel subdivisions.

The nonlinear results for problems in plane Poiseuille flow confirm that certain flows that are stable according to linear theory become unstable to finite amplitude disturbances. The curve relating Reynolds number to critical amplitude indicates the existence of an absolute critical Reynolds number below which the disturbance cannot be made unstable, no matter how large its initial amplitude. This curve also exhibits the behaviour characteristic of equilibrium amplitudes. Our computed critical curve shows significantly less effect of amplitude than do those obtained by earlier workers using perturbation and other asymptotic methods.

The various perturbation and other asymptotic methods used in hydrodynamic stability studies tax the ability of the most able workers and often yield results which are difficult to interpret. Hence there have been numerous failures and disagreements among the various workers in the field even for the relatively simple linear case. The method presented here seems to be the first for which there is a satisfactory error estimate and satisfactory efficiency for nonlinear problems of moderate to large amplitudes. Work of the type presented here should be useful in resolving issues concerning the validity of the various approximation methods, as well as in providing basic information on stability and the early stages of turbulence.

This work was supported by a grant from the Chevron Research Company and by National Institutes of Health Grant HE 09251-06.

REFERENCES

BETCHOV, R. & CRIMINALE, W. O. 1967 *Stability of Parallel Flows*. Academic.

CHANDRASEKHAR, S. 1961 *Hydrodynamic and Hydromagnetic Stability*, p. 634. Oxford University Press.

DAVEY, A. & NGUYEN, H. P. F. 1971 Finite-amplitude stability of pipe flow. *J. Fluid Mech.* **45**, 701–720.

DIXON, T. N. & HELLUMS, J. D. 1967 A study on stability and incipient turbulence in Poiseuille and plane Poiseuille flow by numerical finite-difference simulation. *A.I.Ch.E. J.* **13**, 866–872.

DOWELL, E. H. 1969 Non-linear theory of unstable plane Poiseuille flow. *J. Fluid Mech.* **38**, 401–414.

ECKHAUS, W. 1965 *Studies in Non-linear Stability Theory*. Springer.

GEORGE, W. D. 1970 Application of finite-difference method to the study of non-linear problems in hydrodynamic stability. Ph.D. thesis in Chemical Engineering, Rice University, Houston, Texas.

LIN, C. C. 1955 *The Theory of Hydrodynamic Stability*. Cambridge University Press.

MEKSYN, D. & STUART, J. T. 1951 Stability of viscous motion between parallel plates for finite disturbances. *Proc. Roy. Soc.* A **208**, 517–526.

PEKERIS, C. L. & SHKOLLER, B. 1969*a* Stability of plane Poiseuille flow to periodic disturbances of finite amplitude. *J. Fluid Mech.* **39**, 611–627.

PEKERIS, C. L. & SHKOLLER, B. 1969*b* The neutral curves for periodic perturbations of finite amplitude of plane Poiseuille flow. *J. Fluid Mech.* **39**, 629–639.

REYNOLDS, W. C. & POTTER, M. C. 1967 Finite-amplitude instability of parallel shear waves. *J. Fluid Mech.* **27**, 465–492.

THOMAS, L. H. 1953 The stability of plane Poiseuille flow. *Phys. Rev.* **91**, 780–783.